

This is a repository copy of *Optimization of double pulse pumping for Ni-like Sm x-ray lasers*.

White Rose Research Online URL for this paper:  
<http://eprints.whiterose.ac.uk/1730/>

---

**Article:**

Lin, J Y, Tallents, G J [orcid.org/0000-0002-1409-105X](https://orcid.org/0000-0002-1409-105X), Smith, R et al. (11 more authors) (1999) Optimization of double pulse pumping for Ni-like Sm x-ray lasers. *Journal of Applied Physics*. pp. 672-675. ISSN 0021-8979

<https://doi.org/10.1063/1.369201>

---

**Reuse**

Items deposited in White Rose Research Online are protected by copyright, with all rights reserved unless indicated otherwise. They may be downloaded and/or printed for private study, or other acts as permitted by national copyright laws. The publisher or other rights holders may allow further reproduction and re-use of the full text version. This is indicated by the licence information on the White Rose Research Online record for the item.

**Takedown**

If you consider content in White Rose Research Online to be in breach of UK law, please notify us by emailing [eprints@whiterose.ac.uk](mailto:eprints@whiterose.ac.uk) including the URL of the record and the reason for the withdrawal request.

# Optimization of double pulse pumping for Ni-like Sm x-ray lasers

J. Y. Lin, G. J. Tallents,<sup>a)</sup> and R. Smith

*Department of Physics, University of Essex, Colchester, CO4 3SQ, United Kingdom*

A. G. MacPhee

*School of Mathematics and Physics, Queen's University of Belfast, Belfast BT7 1NN, United Kingdom*

E. Wolfrum and J. Zhang

*Clarendon Laboratory, Department of Physics, University of Oxford, Oxford, OX1 3PU, United Kingdom*

G. Eker

*Department of Physics, University of Essex, Colchester, CO4 3SQ, United Kingdom*

R. Keenan and C. L. S. Lewis

*School of Mathematics and Physics, Queen's University of Belfast, Belfast BT7 1NN, United Kingdom*

D. Neely

*Central Laser Facility, Rutherford Appleton Laboratory, Chilton, Oxon, OX11 0QX, United Kingdom*

R. M. N. O'Rourke

*School of Mathematics and Physics, Queen's University of Belfast, Belfast BT7 1NN, United Kingdom*

G. J. Pert

*Department of Physics, University of York, York, YO1 5DD, United Kingdom*

S. J. Pestehe

*Department of Physics, University of Essex, Colchester, CO4 3SQ, United Kingdom*

J. S. Wark

*Clarendon Laboratory, Department of Physics, University of Oxford, Oxford, OX1 3PU, United Kingdom*

(Received 3 August 1998; accepted for publication 15 October 1998)

We report a systematic study of double pulse pumping of the Ni-like Sm x-ray laser at 73 Å, currently the shortest wavelength saturated x-ray laser. It is found that the Sm x-ray laser output can change by orders of magnitude when the intensity ratio of the pumping pulses and their relative delay are varied. Optimum pumping conditions are found and interpreted in terms of a simple model. © 1999 American Institute of Physics. [S0021-8979(99)07102-9]

## I. INTRODUCTION

Maximizing the efficiency of generating x-ray lasers reduces the driving energy required to produce shorter wavelength x-ray lasing. Using double drive pulses (one prepulse and one main pulse) to pump x-ray lasers has been shown to be able to saturate x-ray laser output of Ni-like Ag (14 nm),<sup>1</sup> In (12.6 nm),<sup>2</sup> Sn (12 nm),<sup>3</sup> and Sm (7.3 nm)<sup>4</sup> at plasma medium lengths 18–20 mm. With double pulse pumping, the first pulse produces cold plasma from the solid. During the time interval between the prepulse and main pulse, the preformed plasma expands and forms a long scale-length electron density profile. The longer scale-length plasma not only increases the energy absorption of the plasma from the driving laser (main pulse) via inverse Bremsstrahlung absorption, but also produces less refraction of the x-ray laser beam and better propagation within the gain region. Previous studies<sup>5–7</sup> suggest that the level of prepulse irradiance and the pulse interval between the prepulse and main pulse determine the electron and ion temperatures, the electron den-

sity gradient, the laser gain, and the maximum x-ray laser propagation distance in the plasma and that these parameters control the x-ray laser output.

In this article, we have made a systematic experimental study of double pulse pumping of the Ni-like Sm x-ray laser at 7.3 nm. The Ni-like Sm x-ray laser has been successfully demonstrated as the shortest wavelength saturated x-ray laser achieved in the laboratory.<sup>4</sup> To determine the optimum double pulse pumping configuration, double pulses with various pulse ratios (the ratio of the irradiance of the prepulse to main pulse) and pulse intervals (the time between the prepulse and main pulse) were irradiated on single Sm slab targets. The targets were of 14 mm length which is sufficiently short to avoid the laser operating in the saturation region during the optimization procedures. We expect the gain length product from a single 14 mm target is  $\leq 13$ .<sup>4</sup>

## II. EXPERIMENTAL ARRANGEMENTS

The experiment was carried out at the Rutherford Appleton Laboratory using the Vulcan Nd-glass laser at 1.05 μm. Before entering the preamplifiers of the Nd-glass laser chain, the stretched oscillator pulse with a pulse duration of ~75 ps was divided by a beam splitter to produce double pulses with

<sup>a)</sup>Electronic mail: tallg@essex.ac.uk

adjustable pulse intervals. While keeping the irradiance of the second pulse (main pulse) at the same level, the first pulse's irradiance was controlled by inserting pre-calibrated filters to produce the required pulse ratio (prepulse/main pulse). After the amplifier chain, each of the Vulcan laser beams could deliver up to 22 J (in the main pulse) on the target. Three beams were overlapped onto the target in a 19 mm×75 μm width line focus by using a combination of three *f*/2.5 spherical lenses and three *f*/2.5 off-axis spherical focusing mirrors to produce a peak irradiance of the main pulse on the target of up to  $\sim 6 \times 10^{13}$  W/cm<sup>2</sup>.

The ratio of the prepulse to main pulse irradiance was monitored by two fast photodiodes in the laser control area and was double checked by a fast vacuum diode in the target area. For shots with high pulse contrast ( $> 10^2$ ), one photodiode with less filtering was arranged deliberately to be saturated by the main pulse to provide a measurable prepulse signal level for comparison with the main pulse signal measured by the other photodiode.

The targets were 14 mm long flat slabs consisting of 75 μm width and 1–2 μm thickness samarium stripes coated on glass substrates. The primary on-axis diagnostic was a grazing angle flat field spectrometer with a 1200 lines/mm aperiodically ruled grating. The spectrometer recorded emission from 60 to 240 Å wavelength and from –1 to 11 mrad angular deviation in the horizontal direction (perpendicular to the target surface) on an InstaSpec IV back-thinned soft x-ray charge coupled device (CCD) detector. The collection angle  $\sim 1$  mrad of the spectrometer in the vertical direction is limited by the entrance slit. Thin Ag, Al, and C filters were used to eliminate optical light and attenuate the lasing signal to adequate levels at the CCD detector. The absolute laser output is calculated by integrating (over wavelength and angle) the lasing signal on the CCD detector and taking into account the filter transmission, the grating reflectivity (measured using synchrotron radiation  $\cong 10\%$ ),<sup>8</sup> and the estimated fraction ( $\sim 1/6$ ) of laser photons collected in the vertical direction. The uniformity and the ionization balance along the line focus was monitored by a space-resolving and time-integrating Bragg crystal spectrometer with a 300 mm convex curvature potassium acid phthalate (KAP) crystal ( $2d = 26.64$  Å). An attached CCD detector recorded the resonance line emissions from 7 to 11 Å. For some shots, another crystal spectrometer with a 300 mm curvature KAP crystal was coupled to an x-ray streak camera to measure the time-resolved ionization balance from the lasing plasma media. The width of the timing slit of the streak camera was set to be 200 μm, which gave a temporal resolution  $\sim 20$  ps.

### III. RESULTS

Figure 1 shows a typical on-axis time integrated spectrum of the lasing signals from a 14 mm long Sm target. The lasing spectrum is dominated by the *J*=0–1 transition at 73 Å, seen in three orders, while the other transition line at 68 Å is also visible. To determine the best pump pulse configuration for the Ni-like Sm laser, a series of shots using various pulse ratios and pulse intervals were carried out. Keeping the peak irradiance of the main pulse consistently at  $\sim 5$

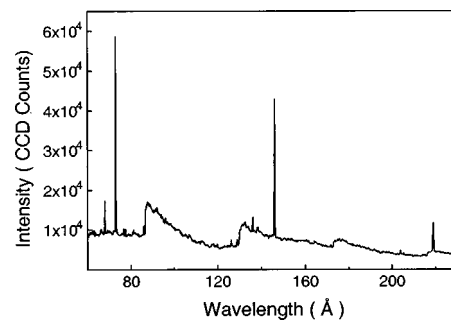


FIG. 1. Axial spectrum from a single 14 mm long Sm target irradiated by double 75 ps pulses with a pulse ratio of 5% and a pulse interval of 2.2 ns. The first order of the lasing line at 73 Å is slightly saturated in the CCD detector.

$\times 10^{13}$  W/cm<sup>2</sup> (with less than a 10% energy fluctuation), the x-ray laser output for each pulse interval is found to peak at various pulse ratios (Fig. 2). A lower level of prepulse is optimal as the pulse interval is increased. Pumping with the optimum pulse ratio increases the laser output by orders of magnitude compared with unoptimized pulse ratios and pulse intervals.

The brightest Sm x-ray laser has been observed using a 0.5% prepulse with a pulse interval of 3.5 ns, but the maximum optimized x-ray laser output with pulse intervals of 2.2, 3.5, and 5 ns differ by less than a factor of 2 (Fig. 2). However, a 1 ns pulse interval gives a factor 4–7 less signal than that of the optimized laser output for the other pulse intervals.

The beam quality of the brightest Sm x-ray laser pumped by double pulses with a 1 ns pulse interval was found to be similar to those pumped by double pulses with 2.2, 3.5, and 5 ns pulse intervals. The divergence (full width at half maximum) and deflection angle (beam pointing angle relative to the target surface) of the x-ray laser beam were measured to be  $2.5 \pm 1$  and  $5 \pm 1$  mrad, respectively, as shown in Fig. 3. These values are small because of the lack of significant refraction effects in the Ni-like Sm x-ray laser. The short wavelength and flat electron density profiles smoothed by the prepulse mean that refraction is small.

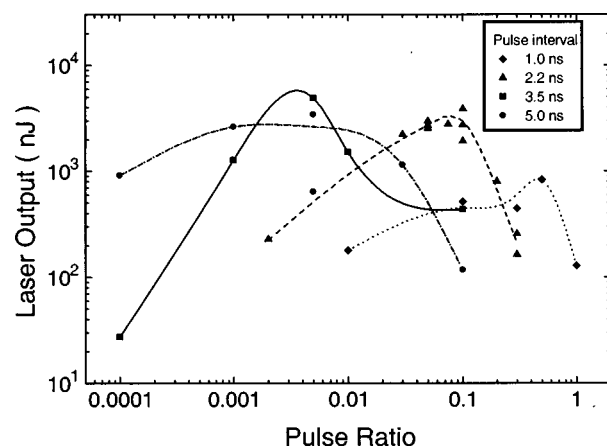


FIG. 2. Variations of x-ray laser outputs at 73 Å as a function of the pulse ratio for various pulse intervals. The peak irradiance of the main pulse is at  $\sim 5 \times 10^{13}$  W/cm<sup>2</sup>.

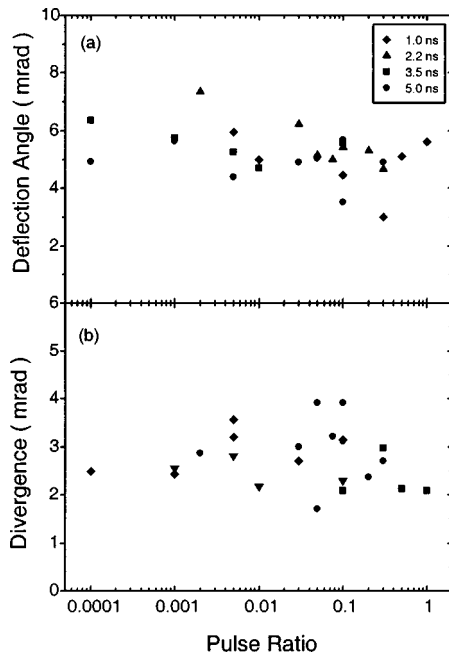


FIG. 3. (a) Deflection angle, and (b) divergence of the Sm x-ray laser as a function of the pulse ratio for various pulse intervals.

The degree of ionization of the x-ray lasing plasma was monitored by a keV crystal spectrometer. As the temperature rises in the plasma, we expect more Co-like and higher ionization stage ions to be generated and consequently stronger band emissions from those ionization stages. A comparison of time-integrated Sm keV spectra pumped by various pulse ratios with a 3.5 ns pulse interval had been made during the experiment. Experimental observations suggest that Ni-like  $4f-3d$  emissions show no significant variations, when different pulse ratios are used. However, the Co-like  $4f-3d$  emissions, and Fe-like and Mn-like band emissions are significantly lower when a small (0.01%) or large (10%) prepulse is used. The spectra of the Sm x-ray laser medium pumped by an optimum level of prepulse (0.5%) implies a hotter plasma because of the strong emission from the higher ionization stages. Higher temperature in the lasing medium produces a higher excitation rate and thus higher gains.

A typical time-resolved resonance emission of Sm plasma recorded by the streaked keV crystal spectrometer is shown in Fig. 4. The main driving pulse irradiance is shown schematically in Fig. 4 assuming that the start of emission corresponds to the start of the laser pulse. In Fig. 4,  $4f-3d$  band emissions from the Mn-like and Fe-like ionization stages peak slightly earlier than similar emission from the Co-like and Ni-like stages. There is also a significant difference of the emission duration from various ionization stages. The duration [full width at half maximum (FWHM)] of the Mn-like and Fe-like resonance emissions is  $\sim 65$  ps, which is comparable with the duration of the pumping pulse. In contrast, the resonance emissions from Co-like and Ni-like ions last  $\sim 85$  and  $\sim 100$  ps, respectively. The Co-like and Ni-like emissions peak later and last longer probably because of recombination from higher ionization stages after the main drive pulse has switched off.

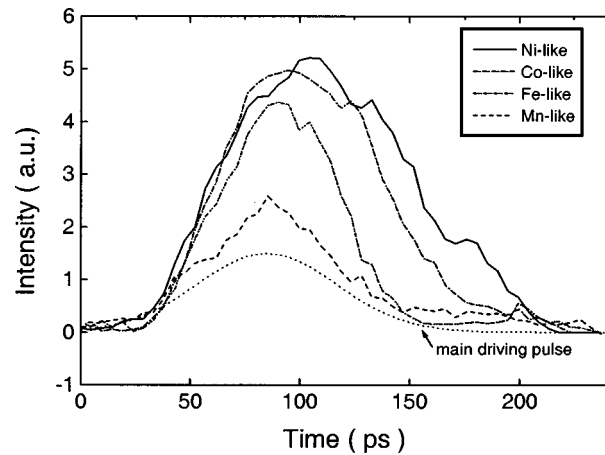


FIG. 4. The time-resolved  $4f-3d$  band emissions of Sm from different ionization stages pumped by a double 75 ps pulse with a 0.1 pulse ratio and a 2.2 ns pulse interval. The main laser pulse irradiance is shown schematically as a dotted line.

#### IV. DISCUSSION

An optimum pulse ratio for x-ray laser output occurs because of a balance between the achieved gain coefficient, the volume of the gain region, and refraction effects. A small prepulse tends to produce a small volume of preplasma. Although this produces a high peak temperature and thus high peak gain coefficient when the preplasma is heated by the main pulse, the gain region is small and refraction effects are serious because of the small volume of plasma produced and steep electron density profiles. In contrast, a too large prepulse gives a larger gain region and less refraction in the plasma, but the peak gain is low. It is also found that the optimum pulse ratio decreases with increasing pulse interval (Fig. 5). A longer pulse interval implies a longer time for the preformed plasma to expand. Although a large scale-length plasma gives a shallower electron density profile, the peak temperature is lower because the main pulse energy has to heat up a larger volume of low-temperature plasma. Hence, a

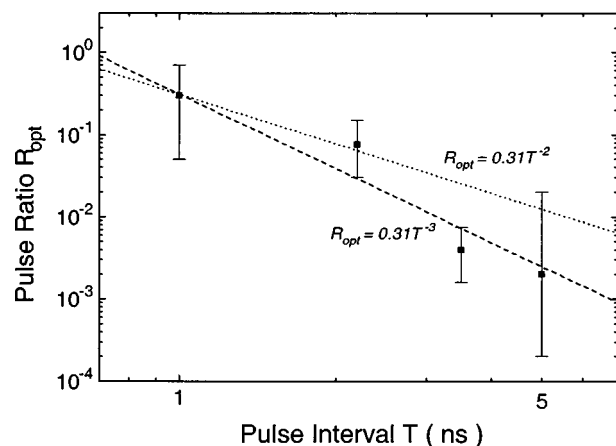


FIG. 5. The pulse ratios  $R_{\text{opt}}$  for optimum x-ray laser output as a function of the pulse interval  $T$ . The error bars show the range of  $R$  giving a factor of 2 variation of x-ray laser output. The curves show a variation of  $R_{\text{opt}}$  scaling according to  $R_{\text{opt}} \propto T^{-2}$  (as for Ref. 5) or  $R_{\text{opt}} \propto T^{-3}$  (the best fit value).

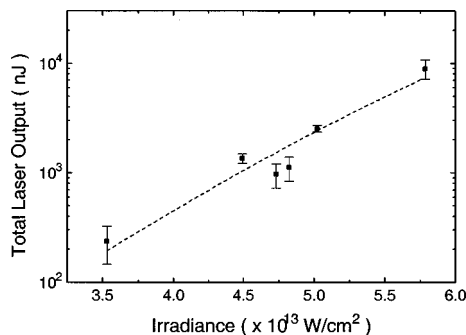


FIG. 6. Sm x-ray laser output as a function of the peak irradiance of the main pulse. The pulse ratio and pulse interval are fixed at 5% and 2.2 ns, respectively. The fitted curve is the expected variation of x-ray laser output taking account of the variation of the collisional excitation rate.

lower level of prepulse is preferred to keep the plasma at a high temperature to produce gains when a long pulse interval is used.

Simulations<sup>6</sup> suggest that the plasma condition of collisional excitation x-ray lasers pumped by double pulses can be quantified by a parameter, the energy density ( $T_e/V_{pre}$ ), where  $V_{pre}$  is the volume of the preplasma just before the arrival of the main pulse and  $T_e$  is the peak electron temperature during the main pulse irradiation. A higher energy density than the optimum value implies over ionization or a narrow gain region with steep electron density gradients, while a lower energy density than the optimum gives low gain and thus lower laser output. By assuming the density profile is determined by the prepulse because of the relatively long pulse interval compared with the driving pulse duration and the preplasma undergoes a two dimensional expansion, the volume of the preplasma can be represented as  $V_{pre} \sim \nu^2 T^2$ , where  $\nu$  is the ionic sound speed and  $T$  is the pulse interval. Since the mass ablation and thus the number of electrons produced by the prepulse are proportional to  $\nu \cdot t$ , the lasing electron temperature is then proportional to  $T_e \propto I_{main}/\nu \cdot t$ , where  $t$  is the prepulse duration and  $I_{main}$  is the peak irradiance of the main pulse. If we assume the ionic sound speed is proportional to  $I_{pre}^a$ , where  $I_{pre}$  is the peak irradiance of the prepulse and  $a$  is a constant, the energy density can be represented as  $T_e/V_{pre} \propto I_{main} I_{pre}^{-3a} t^{-1} T^{-2}$ . Simulations for the Ne-like Ge x-ray laser suggest  $a = 1/3$ , which indicates that the optimum pulse ratio scales as  $(I_{pre}/I_{main})_{opt} \propto t^{-1} T^{-2}$ . In Fig. 5, the best fit optimum pulse ratio scales as  $R_{opt} \propto T^{-3}$ , but  $R_{opt} \propto T^{-2}$  produces a reasonable fit to the experimental results, particularly for pulse intervals  $T \leq 2.2$  ns.

The x-ray laser output increases as the peak irradiance of the main pulse increases (Fig. 6). This can be shown to be due to the increase in electron temperature with increasing irradiance. The collisional excitation rate into the upper

quantum state of the x-ray lasing transition is approximately proportional to  $\sim \exp(-\Delta E/kT_e)/(kT_e)^{0.5}$ .<sup>9</sup> If we assume that the electron temperature is proportional to  $I_{main}/I_{pre}^a$  as above, the gain coefficient is then proportional to  $\exp(-b I_{main}^{a-1})/I_{main}^{(1-a)/2}$ , where  $b$  is a constant. Since the refraction of x-ray lasers is not serious when using a prepulse, the x-ray laser output increases as the exponent of the gain coefficient. After fitting this dependence to the experimental data (see Fig. 6),  $a$  is determined as  $0.35 \pm 0.05$ , which is consistent with the value described above. If we assume the prepulse energy is mainly deposited at the critical density, a simple balance of the pressure  $P \times$  velocity  $\nu$  and laser irradiance at the critical density gives an ionic acoustic velocity  $\nu \propto I_{pre}^{1/3}$ , which also agrees with the scaling value.

### V. CONCLUSIONS

The Ni-like Sm x-ray laser pumped by double drive pulses has proven to be an efficient and bright x-ray source at short wavelength. We have demonstrated the first detailed parameter scan of a double pulse pumped Ni-like x-ray laser using a single Sm target. Using an optimum pulse configuration has been shown to increase the x-ray laser outputs by orders of magnitude. The optimum pulse ratio is found to decrease as the pulse interval increases, which agrees with the predictions of a simple model.

### ACKNOWLEDGMENTS

The authors gratefully acknowledge the assistance of the laser operation and target fabrication staff of the Rutherford Appleton Laboratory. The work has been supported by several grants from the United Kingdom Engineering and Physical Sciences Research Council.

- <sup>1</sup>J. Zhang, A. G. MacPhee, J. Nilsen, J. Lin, T. W. Barbee, Jr., C. Danson, M. H. Key, C. L. S. Lewis, D. Neely, R. M. N. O'Rourke, G. J. Pert, R. Smith, G. J. Tallents, J. S. Wark, and E. Wolfrum, *Phys. Rev. Lett.* **78**, 3856 (1997).
- <sup>2</sup>J. Y. Lin, G. J. Tallents, J. Zhang, A. G. MacPhee, C. L. S. Lewis, D. Neely, J. Nilsen, G. J. Pert, R. M. N. O'Rourke, R. Smith, and E. Wolfrum (submitted).
- <sup>3</sup>J. Zhang, A. G. MacPhee, J. Lin, E. Wolfrum, R. Smith, C. Danson, M. H. Key, C. L. S. Lewis, D. Neely, J. Nilsen, G. J. Pert, G. J. Tallents, J. S. Wark, and P. J. Warwick, *Phys. Lett. A* **234**, 410 (1997).
- <sup>4</sup>J. Zhang, A. G. MacPhee, J. Lin, E. Wolfrum, R. Smith, C. Danson, M. H. Key, C. L. S. Lewis, D. Neely, J. Nilsen, G. J. Pert, G. J. Tallents, and J. S. Wark, *Science* **276**, 1097 (1997).
- <sup>5</sup>G. F. Cairns, C. L. S. Lewis, M. J. Lamb, A. G. MacPhee, D. Neely, P. Norreys, M. H. Key, S. B. Healy, P. B. Holden, G. J. Pert, J. A. Plowes, G. J. Tallents, and A. Demir, *Opt. Commun.* **123**, 777 (1996).
- <sup>6</sup>J. Y. Lin, G. J. Tallents, A. Demir, S. B. Healy, and G. J. Pert, *J. Appl. Phys.* **83**, 1863 (1998).
- <sup>7</sup>S. B. Healy, G. F. Cairns, C. L. S. Lewis, G. J. Pert, and J. A. Plowes, *IEEE J. Sel. Top. Quantum Electron.* **1**, 949 (1995).
- <sup>8</sup>D. Neely, D. Chambers, F. Quinn, and M. Roper, RAL Technical Report, 1997.
- <sup>9</sup>R. C. Elton, *X-ray Lasers* (Academic, London, 1990), p. 101.